ADVANCED FUNCTIONAL MATERIALS
www.afm-journal.de

Materials Views
www.MaterialsViews.com

Manipulating the Hysteresis in Poly(vinyl alcohol)-Dielectric Organic Field-Effect Transistors Toward Memory Elements

*Tzung-Da Tsai, Jer-Wei Chang, Ten-Chin Wen, and Tzung-Fang Guo**

The origins of hysteresis in organic field-effect transistors (OFETs) and its applications in organic memory devices is investigated. It is found that the orientations of the hydroxyl groups in poly(vinyl alcohol) (PVA) gate dielectrics are correlated with the hysteresis of transfer characteristics in pentacene-based OFETs under the forward and backward scan. The applied gate bias partially aligns the orientations of the hydroxyl groups perpendicular to the substrate as characterized by reflective absorption Fourier transform infrared spectroscopy (RA-FTIR), in which the field-induced surface dipoles at the pentacene/PVA interface trap charges and cause the hysteresis. Treating PVA with an anhydrous solvent eliminates the residual moisture in the dielectrics layer, allowing for more effective control of the induced dipoles by the applied gate bias. OFETs of dehydrated-PVA dielectrics present a pronounced shift of the threshold voltage (ΔV_{Th}) of 35.7 V in transfer characteristics, higher than that of 18.5 V for untreated devices and results in sufficient dynamic response for applications in memory elements. This work highlights the usage of non-ferroelectric gate dielectrics to fabricate OFET memory elements by manipulating the molecular orientations in the dielectrics layer.

1. Introduction

Organic field-effect transistors (OFETs) exhibit hysteresis in their transfer characteristics (drain current (I_D) versus gate voltage (V_G) curves), and many research groups have reported the shift of threshold voltage under sequential sweeps.[1–8] The origin of the bias-induced hysteresis in OFETs could be attributed to the use of ferroelectric materials as the gate dielectrics.[9–13] On the other hand, for OFETs made of non-ferroelectric gate dielectrics, the origin of the bias-induced hysteresis is correlated with the trapping of charge carriers in the gate dielectrics,[14–18] the interface at the active layer/dielectrics junction,[19,20] or the active layer[21,22] of devices. The trapped charges electrostatically shield the effective electrical bias applied to the gate with source/drain electrodes, in which the modulations of I_D are associated with the trapping and de-trapping processes of charge carriers[23–25] under the various bias regimes. Due to the instability of I_D at the different sweep of operations[26–28] hysteresis is a serious drawback of OFETs for real applications. However, OFETs with non-volatile bi-stable states of I_D under the programing-erasing bias could be used in applications for memory elements.[29,30] Recent results have successfully demonstrated that the OFETs-based memory elements exhibit the operation voltage levels below 10 V of the potential for real applications.[6,7,8,12,13,18,25]

When used as the gate dielectrics, OFETs made of polymers containing hydroxyl groups (such as the poly(vinyl alcohol) (PVA) or poly(4-vinyl phenol) (PVP)) present pronounced hysteresis in transfer characteristics.[31,32,33,34] Singh et al. fabricated an OFET for memory devices using PVA as a charge-stored gate dielectric.[31] Lee et al. reported that the increase of hydroxyl groups in polymer dielectrics results in an equal increase in the number of trapping sites at the channel/dielectric interface, which causes a large hysteresis.[35] Im et al. and Orgiu et al. demonstrated hysteresis-free OTFT devices by applying PVP and PVA dielectrics with cross-linkers and photosensitizers, respectively.[33,34] It is suggested that the hydroxyl groups could trap charges at the active layer/dielectrics interface, causing hysteresis. Additionally, as reported by Egginger et al., the thermally activated motion of ionic impurities in PVA dielectrics under the influence of applied electrical fields could serve as another parameter to modulate the transfer characteristics of OFETs.[32] The above results indicate that manipulating the hysteresis of PVA- or PVP-dielectrics OFETs is a rather complicated process. The functionalities of hydroxyl groups or moieties in the gate dielectrics should be carefully investigated.

PVA is a polar polymer, having abundant hydroxyl groups attached to polymer chains. The polarity of PVA results from the electrostatic dipoles of hydroxyl groups because of the different levels of electronegativity associated with oxygen and hydrogen atoms. The polarization of hydroxyl groups, such as the orientation or alignment of the dipoles, could be changed by variation of the electrical field (bias). The present study finds that the applied gate bias partially aligns the orientations of hydroxyl groups perpendicular to the substrate (or parallel

T.-D. Tsai, Dr. J.-W. Chang, Prof. T.-F. Guo
Department of Photonics
Advanced Optoelectronic Technology Center
National Cheng Kung University
Tainan, Taiwan 701, ROC
E-mail: guotf@mail.ncku.edu.tw
Prof. T.-C. Wen
Department of Chemical Engineering
National Cheng Kung University
Tainan, Taiwan 701, ROC

DOI: 10.1002/adfm.201203694

© 2013 WILEY-VCH Verlag GmbH & Co. KGaA, Weinheim

to the electrical field) as characterized by grazing-incident reflective absorption Fourier transform infrared spectroscopy (RA-FTIR). Applying a pre-bias at the gate electrode modulates the orientations of the field-induced surface dipoles in PVA dielectrics at the pentacene/PVA interface, which corresponds to the sweep- and moisture-dependent hysteresis in PVA-dielectrics OFETs. We also find that the hydrogen bonding interactions in the PVA offset the influence of the applied electrical field on the re-orientation of hydroxyl dipoles. Through a dehydration process on PVA dielectrics, the shift of threshold voltage in transfer characteristics reaches a maximum with the bi-stable states of I_D under the programing-erasing bias for applications as non-volatile memory elements.

2. Experimental Section

The basic device configuration herein, as presented in inset of **Figure 1**a, comprises a pre-patterned indium tin oxide (ITO)/glass (RITEK Corp.) substrate as the gate electrode that was sequentially coated with a thin layer of poly(3,4-ethylenedioxythiophene):polystyrenesulfonate (PEDOT:PSS Bayer Corp. VP-CH 8000), a crosslinking PVP (Mw = 25 000, Aldrich) layer and a PVA (Mw = 30 000–70 000, Aldrich) layer as the double-layer gate dielectrics, a pentacene active layer, and gold (Au) source-drain electrodes. The low conductivity PEDOT:PSS layer is used to smoothen the roughness of ITO surface, which reduces the gate leakage current, improves the stabilities of devices, and increases the adhesion of PVP layer on the gate electrode. The bottom layer of gate dielectrics was prepared by spin-coating (at 6000 rpm) the PVP (110 mg)/poly(melamine-co-formaldehyde) methylated (40 mg) (Aldrich) in propylene glycol monomethyl ether acetate solution (1 mL) (Aldrich) on the PEDOT:PSS/ITO glass substrate. The substrate was baked at 120 °C for 5 min and then at 200 °C for 20 min to ensure the formation of a cross-linking PVP dielectrics.[36,37] The bottom PVP film has a stable morphology and smooth surface, which is dense to effectively inhibit the gate leakage current. PVA was dissolved in de-ioned water at a concentration of 5.0 wt% and then spun on the surface (at 6000 rpm) of PVP layer as top dielectrics. The chemical structure of PVA is depicted in the inset of Figure 1b. The substrate was baked at 90 °C for 20 min to remove the residual solvent in the dielectrics. The thicknesses of crosslinking PVP and PVA layer were 384 nm and 41 nm, respectively. The pentacene layer (80 nm) (Fluka) and Au electrodes (60 nm) were deposited through a shadow mask on PVA/crosslinking PVP/PDEOT:PSS/ITO glass substrate inside the vacuum thermal evaporator (10^{-6} torr). The complete devices are termed as PVA-dielectrics OFETs in this study. Polystyrene (PS)-dielectrics OFET was made by using PS instead of PVA as the top dielectrics. PS (Mw = 200 000, Aldrich) film was spin-cast from its toluene solution (50 mg/1 mL) at 6000 rpm on PVP surface. All the chemicals were used directly without further purifications. The channel length (L) and width (W) were 100 µm and 1000 µm, respectively. All of these steps for fabrications were implemented inside a nitrogen-filled glove box, except for spin-casting PVA and PEDOT:PSS layers. The moisture and oxygen levels inside the glove box were below 1.0 ppm.

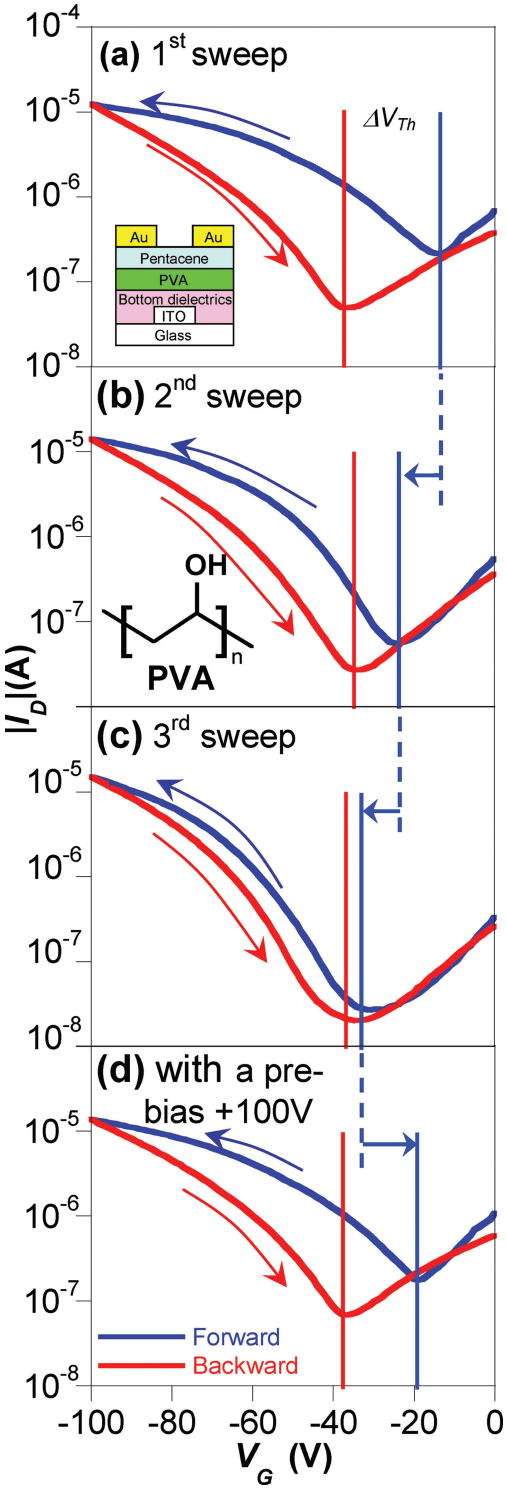

Figure 1. The transfer characteristics (drain current (I_D) versus gate voltage (V_G) curves) of PVA-dielectrics OFETs operated in forward (0 to –100 V) and backward (–100 to 0 V) scans of V_G in successive steps of 1 V with a fixed drain-source voltage (V_{DS}) of –100 V. I_D–V_G curves were taken in the a) 1st sweep, b) 2nd sweep, c) 3rd sweep, and d) when applies a pre-bias of +100 V at the gate electrode for 2 s after the 3rd sweep. The inset of (a) presents the basic OFET configuration herein. The inset of (b) illustrates the chemical structure of the PVA.

© 2013 WILEY-VCH Verlag GmbH & Co. KGaA, Weinheim

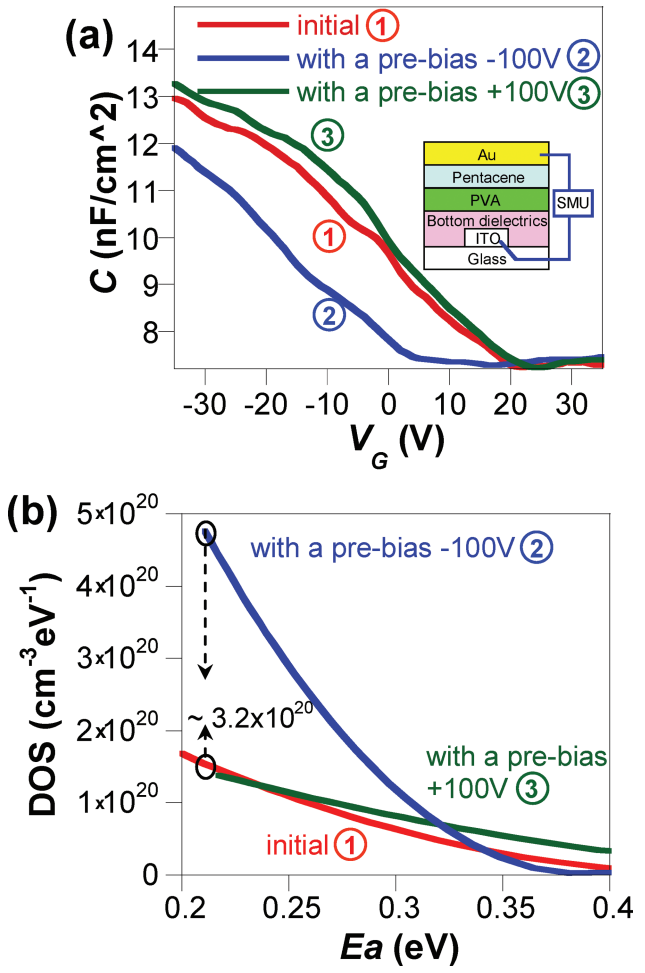

Figure 2. a) *C–V* curves for devices of MIS configuration. The inset illustrates the device of MIS configuration here. b) The DOS versus E_a (for de-trapping) curves for the PVA-dielectrics OFETs. The calculations are based on the model proposed by Kalb et al.[42]

The output and transfer characteristics of OFETs were measured inside the nitrogen-filled glove box using a semiconductor parameter analyzer (HP 4145B, Agilent Technologies). The capacitance-voltage (*C–V*) measurements were conducted with a precision LCR meter (HP 4284A, Agilent Technologies) under the biased voltages (–40–40 V) plus a modulated voltage (100 mV) at a frequency of 100 Hz. The device of metal-insulator-semiconductor (MIS) configuration as shown in the inset of **Figure 2**a is composed of the ITO/glass substrate, a PEDOT:PSS layer, a crosslinking PVP layer and a PVA layer, a pentacene layer, and Au top electrode for the *C–V* measurements. The active area of MIS device for *C–V* measurement is of 2.0 mm^2. RA-FTIR spectra were done by a Vertex 70 spectrometer from Bruker purged with nitrogen gas and equipped with an Advanced Grazing Angle (AGA) accessory and a KRS-5 polarizer from Pike for the grazing incident of a *p*-polarized IR beam. 32 scans were collected with a spectral resolution of 4 cm^{-1} by a mercury-cadmium-telluride detector. An Au-coated (100 nm) glass was used as the reflective substrate for the RA-FTIR measurement. The height image of atomic force microscopy (AFM) was taken by Veeco D5000 in tapping mode.

3. Results and Discussion

Figure 1 presents the transfer characteristics (I_D versus V_G curves) of PVA-dielectrics OFETs operated in forward (0 to –100 V) and backward (–100 to 0 V) scans of V_G in successive steps of 1 V with a fixed V_{DS} of –100 V. Figure 1a depicts the transfer characteristics in the first sweep, exhibiting the pronounced hysteresis of I_D. The magnitude of I_D at the same V_G in the backward scan is smaller than that in the forward scan. As shown in Figure 1a, between the forward and backward scans, the device also exhibits a shift of threshold voltage (ΔV_{Th}) of approximately 20.2 V. However, while PVA-dielectrics OFETs are continuously operated in the second and third sweeps, I_D decreases in the forward scan but only shows a slight change in the backward scan, as illustrated in Figure 1b,c. The reduced I_D in the forward scan comes with the shift of threshold voltage (V_{Th}) to the higher negative gate bias and the decreased ΔV_{Th} in the transfer characteristics. The ΔV_{Th} is 20.2, 10.7, and 5.4 V for I_D–V_G curves in 1st, 2nd, and 3rd sweeps, respectively. After five sweeps, the OFETs show no hysteresis in their transfer characteristics (data not shown here), indicating the sweep-dependent ΔV_{Th} in this study.

Hysteresis in the transfer characteristics of OFETs is associated with the trapping of charge carriers as induced by the gate bias.[38,39] These trapped charges possibly shield the electrical field applied to the gate with source/drain electrodes and reduce the I_D of devices.[40,41] We attribute the sweep-dependent ΔV_{Th} observed in Figure 1a–c to the sequential accumulation of charges in the OFETs under continuous operation. Presumably, these bias-induced charges can be removed by applying an opposite bias or by post-annealing at elevated temperatures. As illustrated in Figure 1d, the I_D–V_G curve was taken for the device (after the third sweep); when applying a pre-bias of +100 V at the gate electrode for 2 s, I_D increases in the forward scan with a shift of the threshold voltage toward the original magnitude of the first sweep, showing a reversible ΔV_{Th} by the gate bias.

To understand the mechanisms that cause the trapping of bias-induced charges, a PS-dielectrics OFET was fabricated for comparison, with its I_D–V_G curves depicted in **Figure 3**. No hysteresis is found in the forward and backward scans of transfer characteristics for the PS-dielectrics OFET. Successive device operations would not change the I_D or shift the threshold voltage, which implies the trapping of charge carriers in the PS-dielectrics OFET is minor compared to that found in the PVA dielectrics OFET. The insets of Figure 3 present AFM height images of pentacene films deposited on PVA and PS dielectrics. The surface morphologies, grain sizes and boundaries, and the roughness of pentacene films for these two samples are quite similar. Therefore, the difference in the intrinsic and electrical properties of the dielectrics layer is responsible for the variations in the PVA- and PS-dielectrics OFETs. The accumulation of charges at the gate dielectrics layer or at the interface between dielectrics/pentacene layers is critical to modulating the output performance of the PVA-dielectrics OFETs.

© 2013 WILEY-VCH Verlag GmbH & Co. KGaA, Weinheim

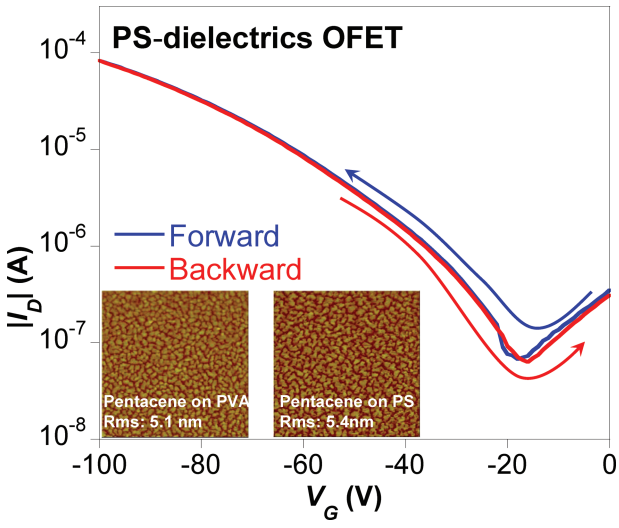

Figure 3. The transfer characteristics of PS-dielectrics OFET in forward and backward scans. The insets present AFM height images of pentacene films deposited on PVA and PS dielectrics.

The influence of trapped charges on device performance is characterized by the quasi-static *C*–*V* measurements. Figure 2a presents *C*–*V* curves for the MIS configuration device (inset of Figure 2a). In the initial measurement, the magnitude of capacitance increases at the negative bias on the ITO/glass electrode, indicating the injection of holes from the Au electrode into the pentacene layer. However, the magnitude of capacitance drops by approximately 15–20% in the MIS device with a pre-bias of –100 V on the ITO/glass electrode for 2 s. This pre-bias causes the trapping of charges in the MIS device, which screens the effective electrical field applied to on the electrodes and reduces the magnitude of capacitance in the *C*–*V* measurements. While a pre-bias of +100 V for 2 s is applied to the ITO/glass electrode, the capacitance recovers to its original magnitude as shown in Figure 2a, possibly because of the de-trapping of charges by the reversed bias.

The density of trap states in the PVA-dielectrics OFETs can be estimated based on the model proposed by Kalb et al.[42] Figure 2b demonstrates the density of trap states (DOS) versus the activation energy (E_a) curves for the PVA-dielectrics OFETs (see Supporting Information for the interpretation and calculation of DOS). The transfer characteristics of PVA-dielectrics OFETs were taken at a low drain voltage of –5 V in a temperature range from 9 to 36°C. The data used to calculate the DOS were taken from the OFETs without any pre-bias and with a pre-bias of –100 V or +100 V at the gate electrode for 2s. Comparing the distributions of trap states shown in Figure 2b, the OFET with a pre-bias of –100 V has a relative higher DOS (about 3.2×10^{20} cm^{-3} eV^{-1} at an activation energy of ≈0.21 eV) than does the device without a pre-bias. The trap states recover to the original distribution after applying a bias at +100 V at the gate voltage for 2 s. Such variations are correlated with the trapping and de-trapping processes of charges in the devices, and agree well with observations of transfer characteristics and *C*–*V* measurements. Since PVA is a polar polymer with abundant hydroxyl groups attached to polymer chains, the polarizations of hydroxyl dipoles would be sensitive to the magnitude and direction of the applied electrical field (bias). Those dipoles near the interface between PVA dielectrics/pentacene layers are critical to trapping (i.e., electrostatically stabilizing) charges, and the polarizations of hydroxyl groups would be important factors in modulating the hysteresis of I_D–V_G curves.

The influence of applied gate bias on the orientations of hydroxyl groups in the PVA layer was studied by measuring the grazing-incident RA-FTIR spectroscopy. The details regarding RA-FTIR can be found elsewhere.[43,44,45,46,47] When a *p*-polarized IR beam comes at an incident grazing angle to the substrate, the absorption for dipole moments oriented normally to the substrate will be significantly enhanced. **Figure 4**c schematically illustrates the principle of RA-FTIR measurement. An increase or decrease in the intensity of a particular IR absorption peak in the RA-FTIR measurement therefore indicates a change in the molecular chain orientation, thus enabling us to determine the average direction of specific dipoles within the PVA chain. **Figure 5**a presents the RA-FTIR spectra of the PVA film on reflective Au-coated glass substrates without and with a pre-bias of –100 V for 2 s. The absorptions of around 2850–2950 cm^{-1} and 3200–3400 cm^{-1} are respectively assigned to the stretching vibrations of C–H and O–H bonds. That peak intensities for C–H stretching are almost identical for the PVA films without and with a pre-bias, which implies the electrical field (pre-bias) has no influence on modulating the average orientations of the C–H bonds in PVA. However, the pre-bias of the PVA film increases the peak intensities by approximately 15% around 3200–3400 cm^{-1}. This observation suggests that the average orientations of O–H bonds in the PVA film are subject to change by the applied electrical field. The pre-bias tends to align the hydroxyl groups (dipole moments) in the PVA film to stand more perpendicularly to the substrate plan (or parallel to the direction of the applied electrical field) than those without the pre-bias. The RA-FTIR spectra of the PVA film on Au-coated glass substrate without a pre-bias, with a pre-bias of –100 V, and a pre-bias of +100 V under a sequential operation are illustrated in Figure S1, Supporting Information. Both the –100 V and +100 V pre-bias can partially align the orientations (in the opposite direction) of hydroxyl dipoles in the PVA film and modulate the peak intensities of O–H bonds in RA-FTIR spectra.

It is anticipated that, as induced by gate bias, the standing dipoles in PVA near the dielectrics/pentacene junction would assist the trapping of charges in the OFETs. Figure 4a schematically draws the correlations between the aligned dipoles with trapped charges at the PVA/pentacene interface in the PVA-dielectrics OFETs during operations. At the start of the forward scan of the first sweep, hydroxyl groups attached to polymer chains are randomly oriented and distributed in the PVA film with no preferred directions. However, at the end of the forward scan at a –100 V gate bias, the electrical field partially aligns or rotates hydroxyl groups attached to polymer chains in PVA and generates dipoles which stand perpendicularly to the interface (substrate). These dipoles promote charge trapping or electrostatically stabilize the accumulated charges at the interface. Later, those charges shield the effective electrical field that applied to the gate electrode to decrease I_D, shift the threshold voltage toward a higher magnitude, and cause the hysteresis in

© 2013 WILEY-VCH Verlag GmbH & Co. KGaA, Weinheim

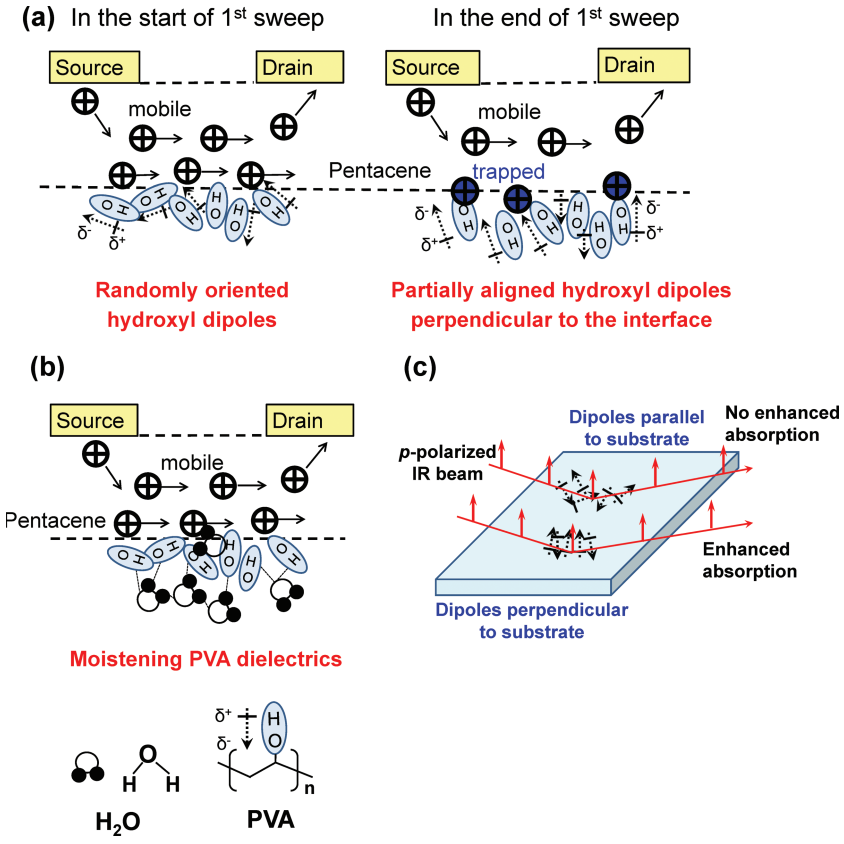

Figure 4. a) A schematic draw for the correlations between the aligned dipoles with trapped charges at the PVA/pentacene interface in the PVA-dielectrics OFETs during operations. The electrical field partially aligns or rotates hydroxyl groups attached to polymer chains in PVA and generates dipoles at the end of the first sweep to promote charge trapping or electrostatically stabilize the accumulated charges at the interface. b) A schematic draw for the mechanism about the influence of the absorbed water molecules to the polarizations of hydroxyl groups attached to the PVA polymer chains in the PVA dielectrics. The hydrogen bonding interactions from water compensate for the influence of the applied gate bias on the orientations and rotations of the hydroxyl groups to diminish the trapping of charges at the dielectrics/pentacene interface. c) A schematic draw for the principle of RA-FTIR measurement. The absorption is significantly enhanced for dipoles oriented perpendicularly to the substrate, when a *p*-polarized IR beam comes at an incident grazing angle to the substrate.

transfer characteristics at the backward scan of the first sweep, as shown in Figure 1a. As a result, the hysteresis of I_D–V_G curves could presumably be modulated by varying the polarizations, concentrations of hydroxyl groups, and the residual moisture level in PVA layer for PVA-dielectrics OFETs.

To verify the abovementioned assumptions, **Figure 6**a–d presents the I_D–V_G curves for the PVA-dielectrics OFETs of the PVA layer containing varied moisture levels. Figure 6a depicts the transfer characteristics, showing pronounced hysteresis with a ΔV_{Th} of 17.9 V for the PVA-dielectrics OFETs made by annealing the spin-cast PVA layer at 90°C for 20 min inside a nitrogen-filled glove box. However, as shown in Figure 6b, if the device was fabricated using the PVA layer as gate dielectrics without annealing, the PVA-dielectrics OFET exhibits no hysteresis in the I_D–V_G curves. In addition, no hysteresis is observed for the device under the continuous sweep of operations. These results suggest that the content of the residual moisture in PVA determines the formation of hysteresis. The OFET fabricated with a "dry" PVA film shows apparent hysteresis in the I_D–V_G curves. On the other hand, placing the device illustrated in Figure 6a inside a glass bell jar for 20 min with a relative humidity above 95% markedly increases the water content in the PVA dielectrics due to the strong hydrogen bonding interactions between the hydroxyl groups in PVA with water molecules. As illustrated in Figure 6c, due to the moistening process, the PVA-dielectrics OFET displays a very small ΔV_{Th} in the I_D–V_G curves as compared to that in Figure 6a. Another approach to verify the role of residual moisture is to post-anneal the device presented in Figure 6b at 90°C for 20 min inside a nitrogen-filled glove box to dehydrate the PVA dielectrics. Figure 6d shows the I_D–V_G curves with an obvious ΔV_{Th} of 14.3 V for the post-annealed PVA-dielectrics OFET, in which the non-annealed device has no hysteresis at all, as shown in Figure 6b. These observations suggest the absorbed water molecules in the PVA dielectrics suppress the hysteresis in the I_D–V_G curves. FTIR spectroscopy results (see Figure S2, Supporting Information) shows the amount of water molecules in the PVA dielectrics decreases with annealing and increases with moistening.

Figure 4b schematically illustrates the mechanism by which the absorbed water molecules influence the polarizations of the hydroxyl groups attached to the PVA polymer chains in the PVA dielectrics. It is anticipated that PVA polymer tends to absorb water through its very strong hydrogen bonds. As shown in Figure 4b, given a certain water content in the OFET's PVA film, the hydrogen bonding interactions compensate for the influence of the applied gate bias on the orientations and rotations of the hydroxyl groups attached to the PVA polymer chains in the PVA dielectrics. This diminishes the trapping of charges at the dielectrics/pentacene interface due to standing dipoles (as depicted in Figure 4a). As shown in Figure 6b,c, a minimal charge screening effect is found inside the PVA-dielectrics OFETs during the forward and backward scan, and no hysteresis is found in the transfer characteristics. Figure 5b presents the RA-FTIR spectra of the PVA film without annealing on a reflective Au-coated glass substrate. No variation is observed in the absorptions around 3200–3400 cm^{-1} (stretching of O–H bonds) for the PVA film, and it was applied with a pre-bias of –100 V for 2 s, as distinct from the result in Figure 5a, which shows an approximately 15% change in the peak intensity by application of the electrical field. The inset of Figure 5b enlarges the region between 2700–3000 cm^{-1}, in which the absorptions around 2850–2950 cm^{-1} assigned to the stretching vibrations of C–H are also unchanged. This observation supports the above assumption that water molecules offset the influence of the

© 2013 WILEY-VCH Verlag GmbH & Co. KGaA, Weinheim

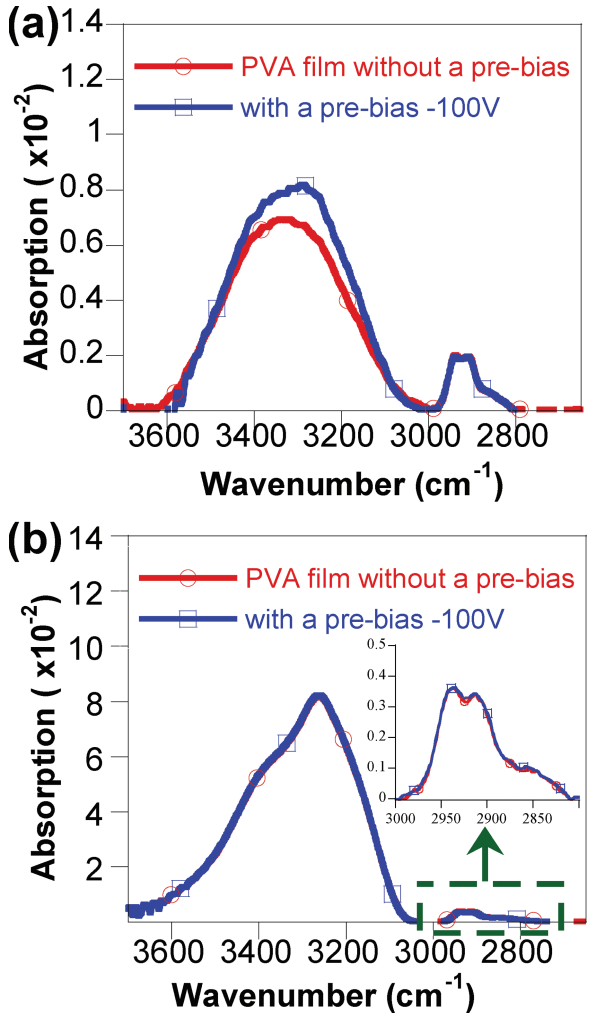

Figure 5. a) RA-FTIR spectra of the PVA film on reflective Au-coated glass substrate without and with a pre-bias of –100 V for 2 s. b) RA-FTIR spectra of the PVA film (no annealing) without and with a pre-bias of –100 V for 2.0 s. The inset of (b) enlarges the region between 2700–3000 cm^{-1} of C–H stretching vibrations.

applied gate bias on the alignment of hydroxyl groups attached to the PVA polymer chains in the PVA dielectrics.

Our result indicates that water molecules in PVA dielectrics diminish the hysteresis in the transfer characteristics. These results are in contrast to previous reports,[29,48,49] in which the residual hydroxyl groups or the amount of water in the dielectrics cause the hysteresis. Since all of steps for fabrication and measurement of devices herein are implemented inside a nitrogen-filled glove box (the moisture and oxygen levels inside the glove box below 1.0 ppm) except for spin-casting PVA, PVP and PEDOT:PSS layers, we exclude the influence of the moisture level in atmosphere and investigate "dry (in a glove box)" and "moistening (under a relative humidity above 95%)" PVA dielectrics on the output performance of OFETs. Figure S2 (Supporting Information) clearly indicate the variations of the water molecules in PVA dielectrics under different conditions. The previous studies for OFETs exhibiting hysteresis in transfer characteristics are observed in a moderately relative humidity about 40% in atmosphere,[48,49] which is a distinct environment to our study. As a result, the concentrations of hydroxyl groups or water levels in atmosphere would also modulate the pronounced hysteresis of OFETs. Additionally, the charges injected from the gate electrode and accumulated in the dielectrics would be another possible mechanism to modulate the hysteresis.[50] We anticipate that the field-induced orientations of hydroxyl dipoles would still dominate the trapping of charges in the "dry" or "moistening" PVA dielectrics/pentacene interface herein and cause the hysteresis.

The polarization or charge accumulation at the PVP/PVA interface is possible. However, the influence from the amount of charges accumulated at the interface between bottom/top (PVP/PVA, PVP/PS) dielectrics or the polarization is relatively small as compared to that in PVA/pentacene interface. Firstly, PS-dielectrics OFETs (of a PVP bottom layer) exhibit no hysteresis in transfer characteristics at all. Secondly, the channel is located at the pentacene layer directly contact to PVA dielectrics. The dipoles or polarizations near in PVA dielectrics/pentacene interface would primarily cause the trapping of charges as well as the hysteresis in the transfer characteristics of PVA-dielectrics OFETs.

As shown in Figure 6, ΔV_{Th} in the transfer characteristics for the PVA-dielectrics OFETs is associated with the amount of water molecules in the PVA layer. Further reducing the amount of residual water would increase ΔV_{Th} of devices for applications in organic memory elements. Accordingly, we propose an approach to dehydrate the PVA dielectrics by immersing the substrate with the PVA film into the anhydrous acetone for 2 minutes followed by blow drying with nitrogen gas in a nitrogen-filled glove box prior to the deposition of the pentacene layer to fabricate the OFETs; the corresponding I_D–V_G curves (forward scan) are illustrated in **Figure 7**a. ΔV_{Th} is 35.7 V in the transfer characteristics for devices measured after programing at V_G = +100 V for 2 s and erasing at V_G = –100 V for 2 s. ΔV_{Th} is 18.5 V for the OFET without the acetone treatment on the PVA dielectrics (data not shown here), which is about half the magnitude of that of the treated device. This result indicates the treatment of anhydrous acetone facilitates the dehydration of PVA film at room temperature and markedly increases ΔV_{Th}.

The dehydrated PVA-dielectrics OFETs are used for applications in non-volatile memory elements. Figure 7c illustrates the dynamic programming-erasing property for the PVA-dielectrics OFETs made of acetone-treated PVA film. The device is programmed at a V_G of 100 V for 5 s, is read at a V_G of –40 V with a drain-source voltage (V_{DS}) of –100 V in ON-state for 1 s, is erased at a V_G of –100 V for 5 s, and is read at a V_G of –40 V with a V_{DS} of –100 V in OFF-state for 1 s. As shown in the bottom part of Figure 7c, the device also can be programmed and erased at a relatively low V_G of 50 and –50 V, respectively. The programming-erasing gate bias results in changes to the magnitude of I_D exhibiting ON-OFF bi-stabilities. The ratio of high- and low-conductance states remains stable through sequential sweeps. Figure 7b shows the time-dependent stability of the conductance in both states. I_D is stable in both the ON-state and OFF-state during prolonged operation, although the value of I_D for these two states slightly decreases at the outset of operations. The difference in the trapping and

© 2013 WILEY-VCH Verlag GmbH & Co. KGaA, Weinheim

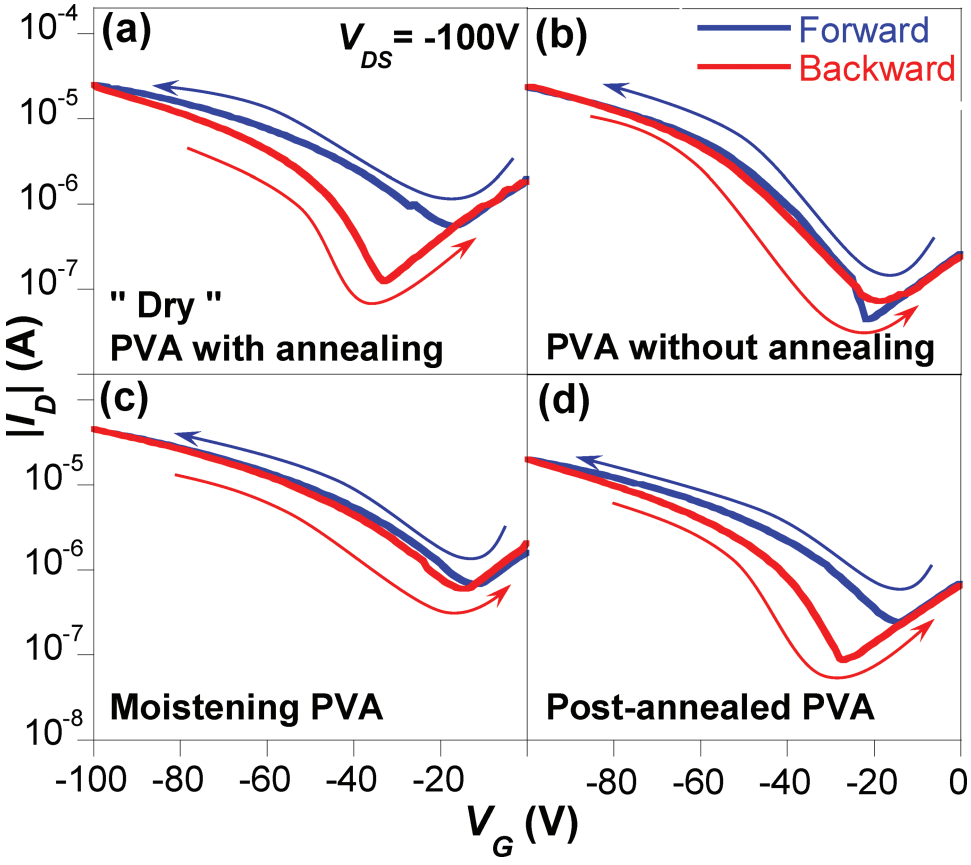

Figure 6. I_D–V_G curves for the PVA-dielectrics OFETs made of a process a) annealing the PVA layer at 90°C for 20 min, b) using the PVA without the annealing, c) placing the device of (a) inside a glass bell jar for 20 min with the atmosphere of the relative humidity higher than 95%, d) post-annealing the device of (b) at 90°C for 20 min inside a nitrogen-filled glove box.

de-trapping of charges at the PVA/pentance interface is seen to cause the variations at the outset of the time-dependent stability in ON- and OFF-states. The stability of I_D in the ON-state and OFF-state or the conductance ratio could be improved by optimizing the interfacial properties at the PVA/pentance junction, such as by modifying the morphology in the pentacene and dielectrics layers or using the gate dielectrics with different functional groups, thus creating a dynamic equilibrium for the trapping and de-trapping of charges currently in progress.

The operation voltage of OFETs and OFETs-based memory elements in this study are relatively high as compared to recent work by others.[6,7,12,13,18,25] This is because the channel length (L) of 100 μm is too long and the thickness of dielectrics layer, PVP and PVA of 384 nm and 41 nm, is too thick herein, which markedly elevate the threshold programming-erasing gate bias for applications in memory elements. This work intends to investigate the origins of the pronounced hysteresis in transfer characteristics of PVA-dielectrics OFETs. We disclose and verify the functionalities of hydroxyl groups in dielectrics layer. We successfully demonstrate the concept to manipulate molecular dipoles in dielectrics layer for fabricating organic memory elements. Applying the device configurations for OFETs, such as devices of 5 to 20 μm channel length with the ultrathin and compact self-assembling dielectrics layer, would significantly reduce the voltage levels. Additionally, the influence of molecular dipoles in dielectrics layer would be critical to the output performance of small dimension OFETs.

4. Conclusion

We report on the cause of the hysteresis of PVA-dielectrics OFETs. The bias-induced re-orientation of the hydroxyl dipoles (as characterized by RA-FTIR) modulate the trapping and de-trapping processes of charge carriers and redistribute the density of trap states at the pentacene/PVA interface. We conclude that the orientation of hydroxyl groups attached to polymer chains in PVA dielectrics are crucial to determining the magnitude of hysteresis, and highlight the usage of non-ferroelectric gate dielectrics to fabricate OFET memory elements. The hydrogen bonding interactions from residual moisture in PVA offset the influence of the applied electrical field on the hydroxyl dipoles. Dehydrating PVA dielectrics through a solvent-treated process allows for more effective manipulation of the bias-induced dipoles. The dehydrated PVA-dielectrics OFET has a maximal shift of threshold voltage in the transfer characteristics, exhibiting non-volatile bistable states of I_D under the programming-erasing bias as used for memory elements.

© 2013 WILEY-VCH Verlag GmbH & Co. KGaA, Weinheim

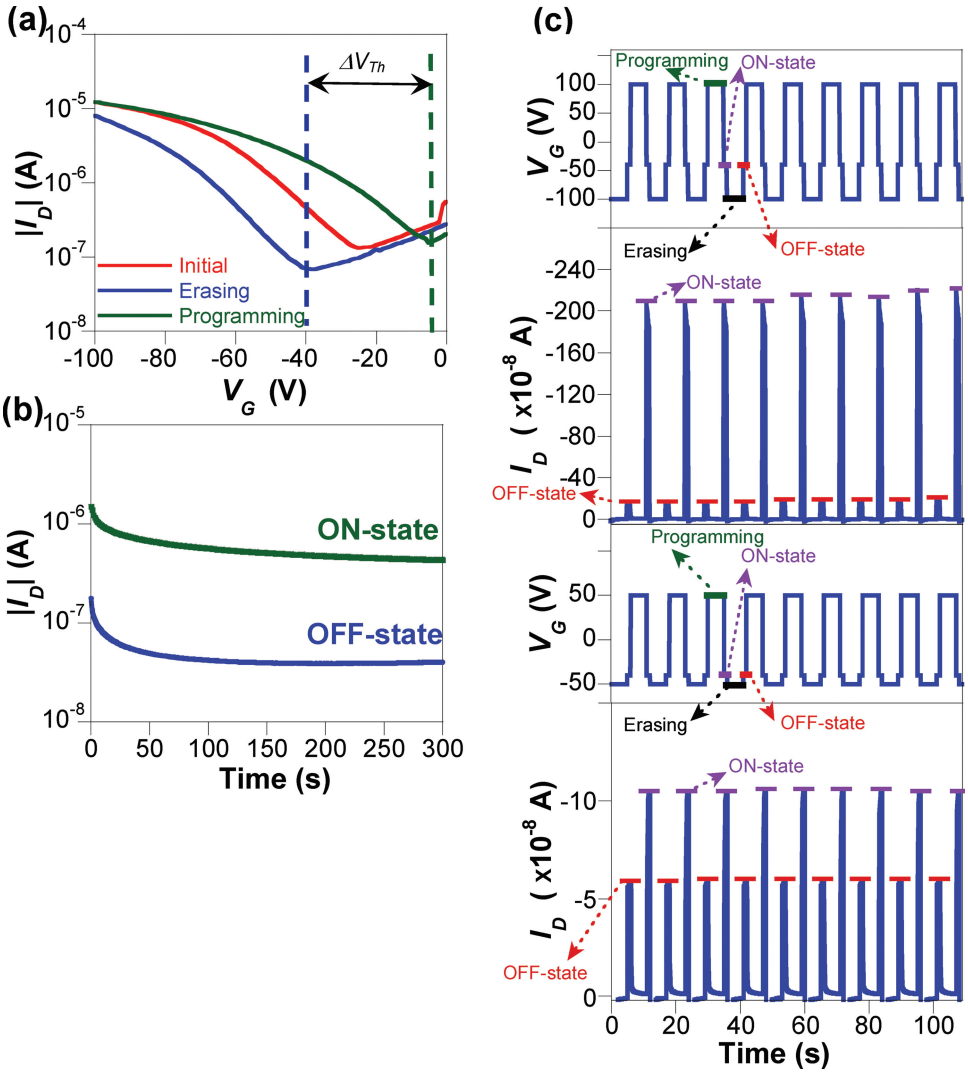

Figure 7. a) I_D–V_G curves (forward scan) of dehydrated PVA-dielectrics OFET at the initial state and under the programing bias at V_G = +100 V for 2 s and erasing bias at V_G = –100 V for 2 s. b) The time-dependent responses of I_D at V_G of –40 V and V_{DS} of –100 V, after programming (V_G of 100 V for 2 s, ON-state) or erasing (V_G of –100 V for 2 s, OFF-state) operations. c) In the upper part, the dynamic programing-erasing responses of the device is programmed at a V_G of 100 V for 5 s, is read at a V_G of –40 V with a V_{DS} of –100 V in ON-state for 1 s, is erased at a V_G of –100 V for 5 s, and is read at a V_G of –40 V with a V_{DS} of –100 V in OFF-state for 1 s. In the bottom part, the dynamic programing-erasing responses of the device is programmed at a V_G of 50 V for 5 s, is read at a V_G of –40 V with a V_{DS} of –50 V in ON-state for 1 s, is erased at a V_G of –50 V for 5 s, and is read at a V_G of –40 V with a V_{DS} of –50 V in OFF-state for 1 s.

Supporting Information

Supporting Information is available from the Wiley Online Library or from the author.

Acknowledgements

The authors would like to thank the National Science Council (NSC) of Taiwan (NSC99-2113-M-006-008-MY3), Asian Office of Aerospace Research and Development (AOARD-10-4054), and NCKU Academic Summit Program for financially supporting this research.

Received: December 14, 2012
Published online: March 26, 2013

[1] J. H. Cho, J. Lee, Y. Xia, B. Kim, Y. He, M. J. Renn, T. P. Lodge, C. D. Frisbie, *Nat. Mater.* **2008**, *7*, 900.
[2] H. Im, X.-J. Huang, B. Gu, Y.-K. Choi, *Nat. Nanotechnol.* **2007**, *2*, 430.
[3] G. Gu, M. G. Kane, *Appl. Phys. Lett.* **2008**, *92*, 053305.
[4] N.-J. Yang, C.-S. Liao, S.-A. Chen, *Adv. Funct. Mater.* **2010**, *20*, 1000.
[5] J. B. Koo, C. H. Ku, S. C. Lim, S. H. Kim, J. H. Lee, *Appl. Phys. Lett.* **2007**, *90*, 133503.
[6] M. Kaltenbrunner, P. Stadler, R. Schwödiauer, A. W. Hassel, N. S. Sariciftci, S. Bauer, *Adv. Mater.* **2011**, *23*, 4892.
[7] R. Nakahara, M. Uno, T. Uemura, K. Takimiya, J. Takeya, *Adv. Mater.* **2012**, *24*, 5212.
[8] T.-W. Kim, H. Choi, S.-H. Oh, G. Wang, D.-Y. Kim, H. Hwang, T. Lee, *Adv. Mater.* **2009**, *21*, 2497.

© 2013 WILEY-VCH Verlag GmbH & Co. KGaA, Weinheim

[9] R. C. G. Naber, C. Tanase, P. W. M. Blom, G. H. Gelinck, A. W. Marsman, F. J. Touwslager, S. Setayesh, D. M. de Leeuw, *Nat. Mater.* **2005**, *4*, 243.
[10] K. H. Lee, G. Lee, K. Lee, M. S. Oh, S. Im, S.-M. Yoon, *Adv. Mater.* **2009**, *21*, 4287.
[11] W. Wu, H. Zhang, Y. Wang, S. Ye, Y. Guo, C. Di, G. Yu, D. Zhu, Y. Liu, *Adv. Funct. Mater.* **2008**, *18*, 3678.
[12] S.-M. Yoon, S. Yang, C. Byun, S.-H. K. Park, D.-H. Cho, S.-W. Jung, O.-S. Kwon, C.-S. Hwang, *Adv. Funct. Mater.* **2010**, *20*, 921.
[13] H. S. Lee, S.-W. Min, M. K. Park, Y. T. Lee, P. J. Jeon, J. H. Kim, S. Ryu, S. Im, *Small* **2012**, *8*, 3111.
[14] K.-J. Baeg, Y.-Y. Noh, J. Ghim, B. Lim, D.-Y. Kim, *Adv. Funct. Mater.* **2008**, *18*, 3678.
[15] C.-C. Chang, Z. Pei, Y.-J. Chan, *Appl. Phys. Lett.* **2008**, *93*, 143302.
[16] M.-F. Chang, P.-T. Lee, S. P. McAlister, A. Chin, *Appl. Phys. Lett.* **2008**, *93*, 233302.
[17] H. Faber, M. Burkhardt, A. Jedaa, D. Kälblein, H. Klauk, M. Halik, *Adv. Mater.* **2009**, *21*, 3099.
[18] M. Burkhardt, A. Jedaa, M. Novak, A. Ebel, K. Voïtchovsky, F. Stellacci, A. Hirsch, M. Halik, *Adv. Mater.* **2010**, *22*, 2525.
[19] K.-J. Baeg, Y.-Y. Noh, J. Ghim, S.-J. Kang, H. Lee, D.-Y. Kim, *Adv. Mater.* **2006**, *18*, 3176.
[20] M. Halik, H. Klauk, U. Zschieschang, G. Schmid, W. Radlik, W. Weber, *Adv. Mater.* **2002**, *14*, 1717.
[21] A. Salleo, R. A. Street, *J. Appl. Phys.* **2003**, *94*, 471.
[22] J. Swensen, J. Kanicki, A. J. Heeger, *Proc. SPIE-Int. Soc. Opt. Eng.* **2003**, *5217*, 159.
[23] W. L. Leong, N. Mathews, S. Mhaisalkar, Y. M. Lam, T. Chen, P. S. Lee, *J. Mater. Chem.* **2009**, *19*, 7354.
[24] K.-J. Baeg, Y.-Y. Noh, H. Sirringhaus, D.-Y. Kim, *Adv. Funct. Mater.* **2010**, *20*, 224.
[25] S.-T. Han, Y. Zhou, C. Wang, L. He, W. Zhang, V. A. L. Roy, *Adv. Mater.* **2013**, *25*, 793.
[26] W. Xu, S.-W. Rhee, *Org. Electron.* **2011**, *12*, 2040.
[27] M. Muoth, T. Helbling, L. Durrer, S.-W. Lee, C. Roman, C. Hierold, *Nat. Nanotechnol.* **2010**, *5*, 589.
[28] M. F. Mabrook, Y. Yun, C. Pearson, D. A. Zeze, M. C. Petty, *Appl. Phys. Lett.* **2009**, *94*, 173302.
[29] D. K. Hwang, M. S. Oh, J. M. Hwang, J. H. Kim, S. Im, *Appl. Phys. Lett.* **2008**, *92*, 013304.
[30] T. Sekitani, T. Yokota, U. Zschieschang, H. Klauk, S. Bauer, K. Takeuchi, M. Takamiya, T. Sakurai, T. Someya, *Science* **2009**, *326*, 1516.
[31] Th. B. Singh, N. Marjanovi , G. J. Matt, N. S. Sariciftci, R. Schwödiauer, S. Bauer, *Appl. Phys. Lett.* **2004**, *85*, 5409.
[32] M. Egginger, M. I. Vladu, R. Schwödiauer, A. Tanda, I. Frischauf, S. Bauer, N. S. Sariciftci, *Adv. Mater.* **2008**, *20*, 1018.
[33] E. Orgiu, S. Locci, B. Fraboni, E. Scavetta, P. Lugli, A. Bonfiglio, *Org. Electron.* **2011**, *12*, 477.
[34] D. K. Hwang, K. Lee, J. H. Kim, S. Im, J. H. Park, E. Kim, *Appl. Phys. Lett.* **2006**, *89*, 093507.
[35] S. Lee, B. Koo, J. Shin, E. Lee, H. Park, H. Kim, *Appl. Phys. Lett.* **2006**, *88*, 162109.
[36] A. L. Briseno, S. C. B. Mannsfeld, M. M. Ling, S. Liu, R. J. Tseng, C. Reese, M. E. Roberts, Y. Yang, F. Wudl, Z. Bao, *Nature* **2006**, *444*, 913.
[37] J.-W. Chang, W.-L. Hsu, C.-Y. Wu, T.-F. Guo, T.-C. Wen, *Org. Electron.* **2010**, *11*, 1613.
[38] W. L. Leong, N. Mathews, B. Tan, S. Vaidyanathan, F. Dötz, S. Mhaisalkara, *J. Mater. Chem.* **2011**, *21*, 5203.
[39] G. Gu, M. G. Kane, S.-C. Mau, *J. Appl. Phys.* **2007**, *101*, 014504.
[40] R. D. Pietro, H. Sirringhaus, *Adv. Mater.* **2012**, *24*, 3367.
[41] G. Gu, M. G. Kane, J. E. Doty, A. H. Firester, *Appl. Phys. Lett.* **2005**, *87*, 243513.
[42] W. L. Kalb, K. Mattenberger, B. Batlogg, *Phys. Rev. B* **2008**, *78*, 035334.
[43] R. G. Greenler, *J. Chem. Phys.* **1966**, *44*, 310.
[44] J. Liu, T.-F. Guo, Y. Yang, *J. Appl. Phys.* **2002**, *91*, 1595.
[45] J. Ouyang, T.-F. Guo, Y. Yang, H. Higuchi, M. Yoshioka, T. Nagatsuka, *Adv. Mater.* **2002**, *14*, 915.
[46] T.-F. Guo, Y. Yang, *Appl. Phys. Lett.* **2002**, *80*, 148.
[47] Y.-T. Tao, *J. Am. Chem. Soc.* **1993**, *115*, 4350
[48] S. H. Kim, S. Nam, J. Jang, K. Hong, C. Yang, D. S. Chung, C. E. Park, W.-S. Choi, *J. Appl. Phys.* **2009**, *105*, 104509.
[49] S. H. Kim, W. M. Yun, O.-K. Kwon, K. Hong, C. Yang, W.-S. Choi, C. E. Park, *J. Phys. D: Appl. Phys.* **2010**, *43*, 465102.
[50] C. A. Lee, D.-W. Park, K.-D. Jung, B.-J. Kim, Y. C. Kim, J. D. Lee, B.-G. Park, *Appl. Phys. Lett.* **2006**, *89*, 262120.

© 2013 WILEY-VCH Verlag GmbH & Co. KGaA, Weinheim